Eur Biophys J (2008) 37:563–571
DOI 10.1007/s00249-008-0262-7

ORIGINAL PAPER

Neutron spin echo studies on ferritin: free-particle diffusion and interacting solutions

Wolfgang Häussler

Received: 13 October 2007 / Revised: 19 December 2007 / Accepted: 21 December 2007 / Published online: 13 February 2008

Abstract The dynamics of proteins are often studied by means of quasielastic neutron scattering (QENS), for example by time-of-flight methods. The spatial dimensions (10–20 nm) present in protein solutions are accessible by neutron scattering. In this article, a systematic study of diffusive dynamics of ferritin and apoferritin (=ferritin without iron core) is presented. Apoferritin consists of a spherical shell built of 24 protein units and carries net negative charge at pH 5. We have studied diffusive dynamics of ferritin solutions by neutron spin echo (NSE). We pay attention to an important feature of this technique compared to other QENS methods, which being the usage of a broad wavelength band. Using a more sophisticated fit function than usually used in NSE, we find as expected in low concentrated systems that the diffusion coefficient approaches the free-particle value of apoferritin and coincides with the diameter of the apoferritin shell (12.2 nm). In interacting solutions, the NSE results reveal that the dynamic picture of this complex liquid is dominated by slowing down of the dynamics. In low-salt solutions, a structure factor peak appears due to ordering of the ferritin molecules on the length scale of several intermolecular distances. We discuss the usage of different NSE fit functions for interacting solutions near the structure factor peak. Comparison of the dependence of elastic and dynamic data on the scattering vector value shows the influence of indirect interactions on the dynamic picture, irrespective of the way of data analysis, which being necessary due to the broad wavelength spectrum.

Keywords Proteins · Neutron spin echo · Diffusive dynamics

Introduction

When biological systems are dissolved in water, so that the interparticle distances are larger than the solved system's diameter, diffusive dynamics appear. Understanding the diffusive dynamics of proteins is fundamental with respect to deeper understanding of the underlying physics and also with respect to the interpretation of measurements of the internal dynamics of proteins. While such measurements have been mostly performed on hydrated powders formerly (Doster et al. 1989), they are now often performed in solution, which means under conditions being comparable to the natural environment of proteins in cells. Concerning the underlying mechanisms, the direct interactions between proteins and their influence on the dynamics are relatively well understood, while the indirect interactions mediated by the solvent are still not completely understood. The latter are based on multi-particle correlations between different proteins, and up to date, there exists no exact theory predicting these interactions. To address this topic experimentally in this article, we systematically investigate solutions of the iron storage protein ferritin showing diffusive dynamics of different complexity, starting with noninteracting solutions and ending with strongly interacting solutions. The hollow protein shell of ferritin, apoferritin (MW = 450–475 kDa, outer diameter 12 nm)

Advanced neutron scattering and complementary techniques to study biological systems. Contributions from the meetings, "Neutrons in Biology", STFC Rutherford Appleton Laboratory, Didcot, UK, 11–13 July and "Proteins At Work 2007", Perugia, Italy, 28–30 May 2007.

W. Häussler (✉)
FRM-II & E21, Technische Universität München,
Garching, Germany
e-mail: wolfgang.haeussler@frm2.tum.de

(Kilcoyne et al. 1992; Häußler et al. 2002), carries a net negative charge at pH ≈ 5 (Petsev and Vekilov 2000), which ensures solubility in water. Moreover, because of electrostatic interactions, ordering over several intermolecular distances has been found, which is reflected in a pronounced peak in the static structure factor $S(q)$ (Häußler et al. 2002). The ferritin shell is highly monodisperse (i.e., identical molecular weight, size, shape and charge of the polyions), which is an advantageous property often found in protein systems in solution or, more general, in systems built by biological molecules in solution. The shape and monodispersity of the ferritin shell facilitates interpretation of the dynamic data with respect to direct and indirect interactions on the dynamic picture of a macromolecular solution.

For the studies on diffusive dynamics of ferritin systems presented here, we employ the neutron spin echo (NSE) technique (Mezei 1980), because this technique matches both the right range of scattering vector and time scale in contrast to earlier studies, which restricted their investigation to low q-values (Petsev and Vekilov 2000; Häußler et al. 2002). Scattering studies of biological particles have to resolve structures on the nanometer scale and are therefore restricted to neutron and X-ray scattering techniques, while the size of synthetic colloidal particles can be controlled by the synthesis process and thus scales of length and time can be adapted to various experimental techniques, for example light scattering (Brown 1996). High-energy resolution is necessary in protein diffusion studies, because the diffusion coefficient is decreasing with increasing radius of the solute. Because the size of ferritin is of several nanometers, diffusive dynamics of ferritin are either at the limit or even beyond the resolution limit for all other neutron scattering techniques: when the scattering vector q corresponds to nanometer-resolution, translational diffusive dynamics are found in the nanosecond time range, as these dynamics scale with the square of the scattering vector q. The only technique suited for revealing a complete picture of the diffusive dynamics of ferritin in solution is the NSE method. Compared to other neutron scattering techniques, it provides the highest energy resolution corresponding to the timescale of several hundreds of nanoseconds. Nevertheless, center-of-mass dynamics influence all quasielastic protein measurements in solution, even on instruments that have resolution lower than nanoseconds, because in the energy domain, the measured data have to be described by a convolution of all sources of dynamics.

The high-energy resolution of NSE is accomplished by the fact that the width of the wavelength band used is decoupled, in principle, from the energy resolution, in contrast to all other methods. In NSE, the wavelength spread does not decrease the measured signal (neutron polarization), but influences the spread of q-values and spin echo times. We describe a theory for special data analysis by means of an exact analytical formula taking into account a triangular wavelength distribution used typically in the NSE technique; so even wavelength spreads as large as 10–20% do not decrease the high NSE resolution, neglecting small deviations from the triangular shape of the wavelength spectrum.

We present results from NSE measurements and partly reexamine data from our earlier work (Häußler 2003) using the exact fit strategy for NSE data, to emphasize the differences between free-particle diffusion and dynamics in interacting solutions. The study is focusing on coherent scattering, as the coherent scattering length difference between the solvent and the hydrogen containing protein gives the dominant contribution to scattering in the q-range near the structure factor peak; so it is most relevant for comparison with other coherent studies. It also shows, however, relevance for "incoherent studies" of biological molecules. In incoherently scattering biological samples, coherent scatterers are present within the incoherent main part of the sample, and a relevant part of the scattering may remain coherent. Often, the dynamic data obtained by quasielastic neutron scattering (QENS) are only corrected for free-particle dynamics. This strategy is correct for the incoherent part of the scattering but not for the coherent part. In this article, we systematically compare coherent dynamics of interacting ferritin proteins with free-particle dynamics detected in incoherent scattering. We find that free-particle diffusion of ferritin is well described by the fit function taking into account the NSE wavelength spread. The dynamics in solutions of higher protein concentration can still be fitted well by the same function. The results show that the diffusive dynamics are mainly decelerated, indicating the existence of indirect interactions. In strongly interacting solutions, the shape of the static structure factor $S(q)$ is reflected in the dynamics [Pusey and Tough 1985]. The slope of $S(q)$ also makes it necessary to verify the validity of the fit function, because of averaging over a broad wavelength band. For the systems at high ionic strength, the influence of indirect interactions slowing down the dynamics compared to free-particle diffusion is quantitatively analyzed, and the dynamics near the structure factor peak in low ionic strength systems is qualitatively studied. Besides the derivation of the NSE fit function in "Theory," the present work is mainly restricted to an experimental study. Comparison of the data with theoretical concepts will be done in future work. The article is organized as follows. "Experimental" describes the steps undertaken for sample preparation and the experimental technique NSE. "Theory" contains the derivation of the theoretical description of dynamics in the case of NSE. "Results and discussion" reports and discusses the NSE results and in "Conclusions" final conclusions are drawn.

Experimental

Samples

Protein solutions (ferritin from horse spleen purchased from Boehringer Ingelheim, Germany and apoferritin from horse spleen purchased from SIGMA, Hamburg, Germany, concentration 51 mg/ml, sodium salt content 100 mM) were dialyzed to solvents of different salt contents as follows: First, the solution was concentrated by a factor of 5–6 by centrifuging small amounts of the stock solution (3 ml) at 8,000 rpm using 10-kD filters (Millipore "Ultrafree", Schwalbach, Germany). Then, 3 ml D_2O was added, followed by a subsequent centrifugation step. To end up with 99.9% deuterated solvent, this was repeated four to five times. Finally, different amounts of pure as well as salty D_2O (NaCl, Riedel de Haen, Hannover, Germany) were added. The protein content was determined by weighing the starting volume of the protein solution before dialysis. The concentration values of the sample solutions used were calculated from the D_2O volume determined by weighing the final solutions. Depending on the apoferritin concentration, pH values are in the range: $5.1 < \mathrm{pH} < 5.3$ (Petsev and Vekilov 2000).

Depending on the final concentration, 1–2 ml of the sample solution was filled into quartz cuvettes (Hellma, Germany, 30×30 mm^2). The sample thickness was 1 mm for the highly concentrated sample and 2 mm for the lower concentrated sample solutions. The transmission through empty cuvettes was 95%; the transmission of the samples was between 69% for the low-concentrated samples (in 2 mm cuvettes) up to 82% for the higher concentrated samples (1 mm cuvettes). The polarization of the scattered intensity normalized by the polarization measured with graphite was at least 0.97. This high value proves that the solvent has been effectively changed to D_2O in all samples, and incoherent scattering from H (and H_2O) can be neglected.

Neutron spin echo measurements

The measurements were performed using NSE instrument IN15 (ILL Yellow Book 2007) at the Institute Laue-Langevin (ILL, Grenoble). The wavelength spread, determined by the wavelength selector, was 17% (FWHM). We used wavelengths of 14.7 and 15.1 Å. The magnetic field integral was 2.7×10^5 Oe cm in maximum. At the given wavelength and field integral, the maximum spin echo time (τ_{SE}) was 190 ns. The maximum value of the beam divergence was 0.17 mrad. The scattering vector covered the range $0.02\ \text{Å}^{-1} < q < 0.1\ \text{Å}^{-1}$. A pixel detector with 32×32 pixels was used, distributed into two to six sections. The sample temperature was 293 K.

The data were corrected for background scattering from the sample cell and solvent. The polarization values extracted from the spin echo measurements as a function of spin echo time were divided by the elastic polarization and corrected for the instrument resolution determined by means of the graphite sample, to obtain the normalized intermediate scattering function.

Theory

Free particle diffusion

The starting point for describing static and dynamic properties of many-particle systems is the coherent intermediate scattering function (Lovesey 1986)

$$I(q,t) \propto \left\langle \sum_{i=1}^{N} \sum_{j=1}^{N} \exp\left(i\mathbf{q}(\mathbf{r}_i(0) - \mathbf{r}_j(t)\right) \right\rangle, \tag{1}$$

where $\mathbf{q}$ is the scattering vector, q its absolute value, N the number of particles in the scattering volume and $\mathbf{r}_i(t)$ is the position of particle i at time t. The brackets denote the equilibrium ensemble average. $I(q) \equiv I(q, 0)$ describes the static structure of the system. For a monodisperse ensemble of spherically symmetric particles, $I(q)$ factorizes as (Pedersen 1997)

$$I(q) \propto F^2(q) \cdot S(q) \tag{2}$$

with the particle form factor $F^2(q)$ and the static structure factor $S(q)$.

In the case of noninteracting particles (dilute protein solutions), $S(q) = 1$ and for classical diffusion of noninteracting spherical particles, the normalized intermediate scattering function

$$S(q,t) = I(q,t)/I(q,0) \tag{3}$$

can been derived by describing the variance of the position of each particle as (Pusey and Tough 1985)

$$\left\langle (r_i(t) - r_i(0))^2 \right\rangle = D_0 t \tag{4}$$

with the Stokes–Einstein free-particle diffusion constant

$$D_0 = \frac{kT}{6\pi\eta a}, \tag{5}$$

where k is the Boltzmann factor, η is the viscosity of the solvent and a is the hydrodynamic radius of the spheres.

Introducing an appropriate Gaussian distribution of a particle performing random walk into Eq. 1 leads to

$$S(q,t) = \exp(-q^2 D_0 t). \tag{6}$$

This theoretical description is based on the assumption that the timescale of the experiment exceeds the short-time

fluctuations of the dissolved particles due to collisions with solvent molecules, an assumption which is justified when the experiment is sensitive to times above the solvent collision time $\tau_S \approx 10^{-12}$ s (Pusey and Tough 1985). The smallest spin echo times used were at least one order of magnitude larger than τ_S.

Interacting solutions

The static structure factor of a solution of interacting proteins is not constant, $S(q) \neq 1$, but shows typical solution structure oscillations. In the case of (almost) spherical proteins like ferritin, the interparticle interactions are isotropic, and $S(q)$ can be computed using Eq. 2 and the form factor amplitude F for a spherical shell, given by (Pedersen 1997)

$$F(q;r_1,r_2) = 3\frac{(\sin(qr_1)-qr_1\cos(qr_1))-(\sin(qr_2)-qr_2\cos(qr_2))}{q^3(r_1^3-r_2^3)} \quad (7)$$

where r_1 is the outer radius of the sphere and r_2 is the inner radius of the sphere. The outer radius r_1 derived by elastic scattering measurements may differ from the dynamic parameter a (see "Results and discussion").

In addition, the dynamics picture is influenced in the case of interacting particles. A rough estimation of the interaction time τ_I needed for a freely diffusing sphere of radius $r_1 = 6$ nm to diffuse through water a distance equal to its radius gives $\tau_I \approx r_1^2/D_0 \approx 1.2$ μs. This time exceeds the maximum spin echo times estimated in this work using the NSE spectrometer (see "Experimental"). Therefore, our NSE study is only sensitive to the apoferritin dynamics taking place in a "short time limit," which means that the diffusive motion of an apoferritin molecule on the time scale of the experiment (several tens of nanoseconds) is not influenced directly by the presence of surrounding proteins, and the first derivative of $S(q,t)$ in a short time limit, describing the initial decay of $S(q,t)$ measured using NSE spectrometer (1 ps $< t <$ 300 ns), can be expressed as (Pusey and Tough 1985)

$$\mathrm{d}S(q,t)/\mathrm{d}t|_{\tau_S<t<\tau_I} = -D_0q^2 \quad (8)$$

being equivalent to $\mathrm{d}[S(q,t)/S(q)]/\mathrm{d}t|_{\tau_S<t<\tau_I} = -(D_0/S(q))q^2$. In the case of (approximately) exponentially decaying processes, to which we restrict ourselves for simplicity reasons, this leads to the following expression for the normalized intermediate scattering function:

$$S(q,t)/S(q) = \exp\left(-(D_0/S(q))q^2t\right) \equiv \exp\left(-D_{\mathrm{eff}}(q)q^2t\right). \quad (9)$$

where we have introduced the effective diffusion coefficient $D_{\mathrm{eff}}(q)$. We note that the influence of indirect interactions, for example hydrodynamic interactions, has been neglected in this derivation.

NSE: usage of a broad wavelength band and detection of free-particle diffusion

In NSE, wavelength spreads as large as 10–20% are typically used, which influence the spread of q-values and spin echo times, but does not restrict the resolution towards high spin echo times (Mezei 1980). The spin echo time τ depends even on the third power of the wavelength λ:

$$\tau = \lambda^3\gamma Jm^2/(2\pi h^2) \quad (10)$$

where γ is the gyromagnetic ratio of the neutron, m its mass, J the magnetic field integral and h Planck's constant. In contrast, q decreases with increasing λ:

$$q = (4\pi/\lambda)\sin(\Theta/2) \quad (11)$$

where Θ is the scattering angle. This, together with Eq. 6, gives the following expression for diffusive dynamics, showing the dependence of $S(q,\tau)$ on λ:

$$S(q,\tau) = \exp\left(-\lambda D_0 8\pi\sin(\Theta/2)^2\Gamma Jm^2/h^2\right) \equiv \exp(-C\lambda) = S(q,\tau(\lambda)) \quad (12)$$

We assume a triangular wavelength distribution function of the width $\Delta\lambda$, centered at λ_0, representing a good approximation for typical NSE wavelength bands generated by neutron velocity selectors. The convolution of the exponential decay (Eq. 12) with this wavelength distribution leads to the final expression (unpublished work):

$$S_{\Delta\lambda}(q_0,\tau) = e^{-C\lambda_0}\frac{2(\cosh(C\Delta\lambda)-1)}{\Delta\lambda^2C^2} \quad (13)$$

where the center value of the scattering vector $q_0 = (4\pi/\lambda_0)\sin(\Theta/2)$. Comparison with Eq. 6 shows that the exponential decay generally used has to be calculated at the mean wavelength using Eq. 10, and then multiplied by a correction factor.

Broad wavelength range and interacting solutions

In the case of interacting solutions, the normalized intermediate scattering function does not show necessarily the same q-dependence as in the case of noninteracting solutions. Firstly, the decay is not necessarily exponential, in general. Secondly, even in the case of an (almost) exponentially decaying intermediate scattering function, the effective diffusion coefficient shows some q-dependence

(Eq. 9), which makes it a function of λ. Therefore, the integration over the wavelength distribution used in NSE cannot be performed in the same way, in general.

However, at almost constant $S(q)$, the integration of Eq. 9 is possible using the expression for the non-normalized intermediate scattering function starting from its derivation given in Eq. 8. In the case of exponential decays, this leads to a similar expression as given in Eq. 12 for noninteracting solutions:

$$S(q,\tau) = S(q)\exp\left(-C\lambda/S(q)\right). \tag{14}$$

If $S(q)$ is (almost) constant over the wavelength range, the integration over the wavelength spectrum can now be performed as described in the previous section and we get

$$S_{\Delta\lambda}(q_0,\tau)/S_{\Delta\lambda}(q_0,0) = e^{-C\lambda_0}\frac{2(\cosh(C\Delta\lambda)-1)}{\Delta\lambda^2 C^2}. \tag{15}$$

$S(q)$ not being constant restricts us to the consideration of the initial decay of $S(q,\tau)$. At small times, $S(q,\tau)$ can be expanded up to first order as

$$S(q,\tau) \approx S(q) - C\lambda, \quad \tau \to 0. \tag{16}$$

This approximate expression can be integrated over the wavelength band, and we get $S_{\Delta\lambda}(q_0,\tau)/S_{\Delta\lambda}(q_0,0) \approx 1 - C\lambda_0/S_{\Delta\lambda}(q_0,0), \quad \tau \to 0$ or, finally

$$S_{\Delta\lambda}(q_0,\tau)/S_{\Delta\lambda}(q_0,0) \approx 1 - D_0/S_{\Delta\lambda}(q_0,0)q_0^2\tau_0, \quad \tau \to 0. \tag{17}$$

Being valid at small spin echo times, Eq. 17 resembles the expansion of an exponential up to the first order, evaluated at the center wavelength or spin echo time. Therefore, in the analysis of data from interacting solutions, Eq. 15 is used for q-values at which the static structure factor is (almost) constant to compare the shape of the data at larger spin echo times with this expression, while the approximate Eq. 17 is used at other q-values, to fit the data at small spin echo times. We also note here that this expression does not take into consideration indirect interactions.

Results and discussion

We start this section with the system showing the simplest dynamic picture, which being the free-particle dynamics, and then subsequently increase interparticle interactions, to detect deviations from free-particle diffusion. Figure 1 displays NSE data acquired from a low concentration apoferritin solution. Interparticle correlations are minimized due to the relatively low concentration of 26 mg/ml. In addition, 21 mM sodium chloride has been added to the solution, to screen the electrostatic forces between apoferritin molecules. Comparison of the NSE data with the theoretical function taking into account the 17% width

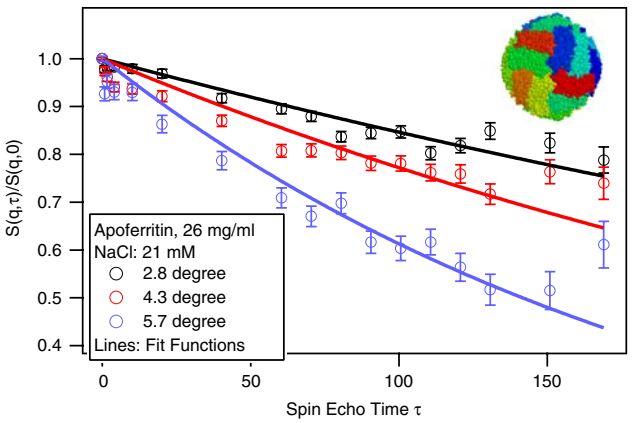

Fig. 1 Normalized intermediate scattering functions acquired by NSE from a solution with (almost) only free-particle diffusion present (apoferritin concentration 26 mg/ml). The fit function (Eq. 13) takes into account the relative wavelength spread of 17% and fits the data very well over almost the whole range of spin echo times measured and for all curves taken at different scattering angles and q-values. At the highest spin echo times, error bars reflecting the statistical error are large as a consequence of low scattered intensity from the low-concentrated solution. When comparing with the fit function, additional systematic errors have to be taken into account (not quantified). They are due to low polarization at the two highest spin echo times, leading to eventually artificially increased polarization values in the spin echo fit. *Inset (top-right)* Sketch of the ferritin molecule, the 24 protein subunits building up the spherical ferritin molecule are displayed in different colors

of the wavelength band (Eq. 13) shows good agreement, except for the largest echo times. Here, the error bars are relatively large, because of the low protein concentration. The count rates are at the limit for being able to acquire data with sufficiently good statistic within reasonable measuring times. In addition, systematic errors influence the data quality (not quantified) due to low polarization at the two highest spin echo times, leading to eventually artificially increased polarization values in the spin echo fit.

NSE data of the lowest concentration system were taken at three different scattering angles and analyzed separately for each angle on three different sections of the pixel detector. Therefore, relaxation rates Γ are available at nine different q-values, and they are displayed in Fig. 2 as a function of q^2. In this representation, they are fitted well by a straight line. This demonstrates that the dynamics is governed by free-particle diffusion, as Γ depends on q as $\Gamma \sim q^2$. The proportional constant derived by the fit yields the diffusion constant of apoferritin in D_2O: $D_0 = 2.8 \times 10^{-7} \pm 0.1$ cm^2/s. The special NSE fit function (Eq. 13) gives here nearly the same result as a simple exponential fit, as shown in the inset of Fig. 2. The diffusion coefficient value is in agreement with the literature value (3.1×10^{-7} cm^2/s), for example with photon correlation spectroscopy data from Häußler et al. (2002) and Gapinski et al. (2005), taking into account the higher viscosity of D_2O

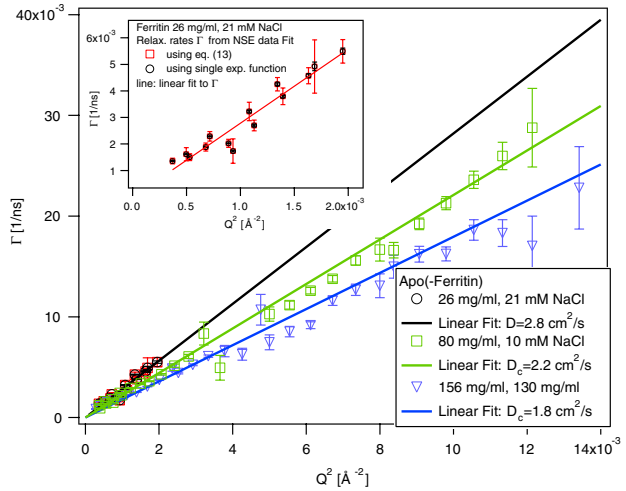

Fig. 2 Relaxation rates Γ as a function of q for the low-concentration sample from Fig. 1 amended by data at different detector sections (see text). The linear shape of the relaxation rate and the fit to a line with the q-dependence $\Gamma \sim q^2$ shows that the data can well be described by the theory of free-particle diffusion. The free-particle diffusion coefficient ($2.8 \times 10^{-7} \pm 0.1$ cm/s) agrees very well with the literature value after scaling the PCS data with a factor due to the difference in viscosity between H_2O and D_2O. Relaxation data of a higher concentrated apoferritin solution shows deviations from free-particle diffusion, as the apparent diffusion coefficient is smaller. The *inset* compares low-concentration data derived in two different ways: by fit using either Eq. 13 (*squares*) or a single exponential function (*circles*). The differences between the fitted relaxation rates are negligible, as the *inset* (*line:* linear fit to relaxation rate data) shows

compared with H_2O. By Eq. 6, the hydrodynamic radius a of apoferritin is calculated to be 6.9 ± 0.2 nm. Both size and shape of the ferritin molecule are well known from literature (Häußler et al. 2002). The form factor has been measured by means of X-ray scattering and neutron scattering (Häußler 2003), and the following numbers derived from these measurements of apoferritin are being used, to compare the dynamic data presented here with the size of the protein known from literature: $r_1 = 6.06 \pm 0.2$ nm, $r_2 = 3.83 \pm 0.2$ nm, $\Delta r_1/r_1 = 4.3\%$ and $\Delta r_2/r_2 = 5\%$; r_1 and r_2, respectively, being the outer and inner radius of the protein shell. The hydrodynamic radius a of ferritin is larger than the form factor radius, because of a hydration shell being present around the molecule in aqueous solution (Harrison and Arosio 1996; Israelachvili and Wennerstroem 1996; Sivergun et al. 1998).

As pointed out earlier, measurements at the relative low protein concentration of 26 mg/ml are intensity limited, especially towards higher q-values. In solutions of higher protein concentration, data of better quality can be acquired and first deviations from free-particle diffusion come into play, which becomes evident from the different slopes of the fits in Fig. 2. The relaxation rates of solutions with apoferritin concentrations of 80 and 156 mg/ml with their respective salt contents 10 and 130 mM differ from the free-particle values. The comparison of the free-particle value with the highest concentration value of 156 mg/ml is of special interest, because the increased salt content compared to the low concentration system decreases the interparticle interactions by screening them. This compensates for the higher protein concentration increasing these interactions. Therefore, direct electrostatic interparticle interactions are of comparable strength in the solution of highest apoferritin concentration and in the low-concentrated solution. The hard sphere interaction remains leading to a well-known maximum in $S(q)$. However, in the q-range under study, $S(q)$ is mainly constant, and Eq. 15 is used for the relaxation rate fits. Moreover, the dynamic data are almost an exact quadratic function of q as seen from Fig. 2. The lower value of the apparent diffusion coefficient reflected by the smaller slope of the linear fit in Fig. 2 compared to the less concentrated system is therefore due to the presence of indirect interactions (Gapinski et al. 2005). We can compare our NSE results to sedimentation measurements (Nägele 2004) corresponding to $q \to 0$. They find that the diffusion coefficient increases with increasing concentration according to $D_{\mathrm{eff}}(q)/D_0 = 1 + 1.454\phi - 0.45\phi^2 + \mathrm{O}(\phi^3)$ with the volume fraction ϕ. In contrast, the diffusion coefficient measured at the NSE q-values decreases with increasing concentration. Though quantitative analysis is difficult for only three concentration values with two fit parameters, by fit of a comparable polynomial function up to second order, we receive the following expression: $D_{\mathrm{eff}}(q)/D_0 \approx 1 - 6.6\phi(-0.3\phi^2)$. We note that the prefactors depend strongly on the diffusion coefficient value at zero concentration (calculated from PCS results in H_2O).

To further increase the interparticle interactions, systems of low salt content are studied. Figure 3 shows relaxation rates measured in three additional ferritin solutions of protein concentrations 80, 117 and 156 mg/ml. To obtain the relaxation rates, the NSE data are fitted with (Eq. 15), as before. The resulting relaxation rate values are fitted to an expression being proportional to q^x. When using data points above 0.03 $\mathrm{Å}^{-1}$, value of 2 is found for the exponent x. This behavior is expected: at high q-values, the part of the intermediate scattering function (Eq. 1) reflecting correlations between different particles cancel out, and only self correlations contribute (Pusey and Tough 1985). With increasing protein concentration, the proportional constant reflecting the apparent diffusion coefficient at high q-values is decreasing, similar to the case of high salt solutions. We mention that the fit curves appear now in Fig. 3 as parallel lines due to the log-log representation used, in contrast to Fig. 2.

A second pronounced deviation from free-particle behavior is visible at low q-values, where the relaxation rates in interacting ferritin solution do not obey a linear dependence of q^2. From Fig. 3, it is seen that at the

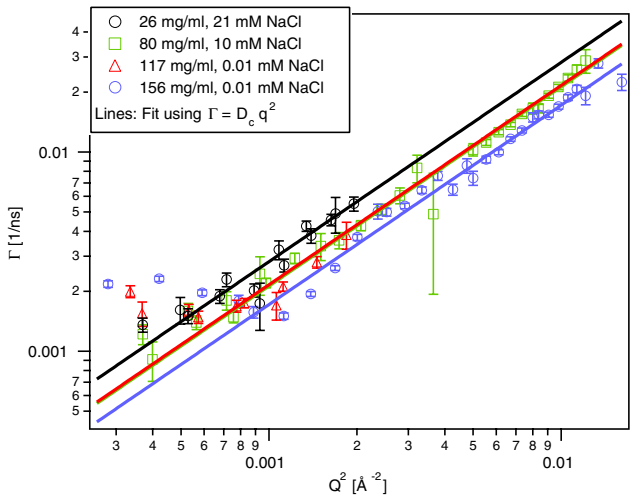

Fig. 3 Relaxation rates measured by NSE in solution with interparticle interactions being present (different apoferritin concentrations as indicated in the figure). The fit functions (Eq. 15) take into account the relative wavelength spread of 17%. At intermediate and high q-values, the relaxation rates are a linear function of q^2, as in the case of free-particle diffusion. However, at low q-values, significant differences appear. The fit functions (*lines*) take into account only data points above 0.03 $Å^{-1}$

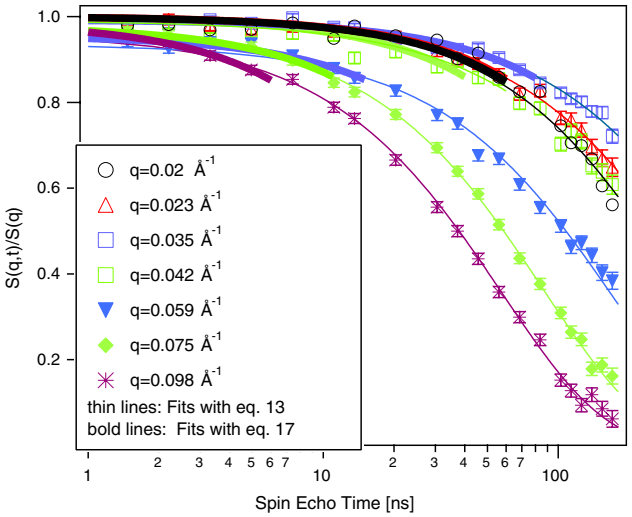

Fig. 4 Normalized intermediate scattering functions measured by NSE in solution with interparticle interactions being present (apoferritin concentration 156 mg/ml). The fit functions take into account the relative wavelength spread of 17%. The *thin lines* represent fit curves received by means of Eq. 15. The *bold lines* represent the fit curves calculated according to Eq. 17, being restricted to low t-values

concentrations of 117 and 156 mg/ml, the relaxation rate is significantly higher at small q-values and lower at intermediate q-values, compared to the fit at high q-values described earlier. The relaxation rate data from the 156 mg/ml solution even start to show a minimum at intermediate q-values. This behavior is expected in systems with strong direct interparticle interactions showing a peak in the static structure factor at this q-value.

Apoferritin solutions are known to show a correlation peak in the static structure factor at low ionic strength (Häußler et al. 2002), and Eq. 15 is not valid any more in the vicinity of the peak (see "Experimental"). To prove that the deviation from the linear fit at small q-values does not depend on the fit function used, these low-salt NSE data were fitted both by the approximate expression taking into account the NSE wavelength spread (Eq. 15) and by the linear expression given in Eq. 17. Figure 4 shows the NSE data for the sample of 156 mg/ml apoferritin concentration and 0.01 mM salt content, together with different fit functions. As the linear fit approximation (Eq. 17) is valid only in the limit $t \to 0$, we have only used those data points, where the normalized intermediate scattering function is >0.86, which means that it has decayed at most by $1 - 0.86 = 0.14$. This guarantees that the error of the approximation is smaller than 1%: the upper limit for the error is the absolute value of the second term of a Taylor expansion, which is $x^2/2$. In our case this is at most $0.14^2/2 = 1\%$, as mentioned earlier.

From Fig. 4, it can be seen that the linear function according to Eq. 17 fits well over the selected range of spin echo times and for all $S(q,t)$ curves at different q-values. Only at the highest spin echo times taken into account for the fit, the linear function starts to deviate slightly from the NSE function fit (Eq. 13), as expected. However, the fit results are slightly different. This difference of the fitted relaxation rates is demonstrated more clearly in Fig. 5 for the 117 mg/ml solution focusing on the small q-range. The reason for the deviations and a more detailed analysis of the result of different fit methods will be the topic of future work. Here, we will finally restrict ourselves to a qualitative analysis of the relaxation data being valid for the results of both fit methods.

Relaxation rate fits acquired by different fit functions from this apoferritin solution (concentration 156 mg/ml) at small and intermediate q-values are shown in Fig. 6 (left). As a result of both fit methods, it turns out that the relaxation rate Γ does not obey the free diffusion dependency $\Gamma \sim q^2$. In the q-range shown, almost all relaxation rate values are found below the free-particle diffusion line added to the plot. However, at low q, the dynamics are faster than that at intermediate q-values. Following the shape to higher q-values, the relaxation starts to follow the line being a function of q^2, as described in detail earlier. Also for the data from the 156 mg/ml solution, the differences between relaxation values obtained from fits with Eqs. 15 and 17 are found to be relatively small and almost in the order of magnitude of the statistical errors. Most pronounced differences are found around $q = 0.042$ $Å^{-1}$ and at the highest q-values shown. The latter difference originates from the fact that at high q-values, the dynamics are almost relaxed (Häußler 2003), and the number of data

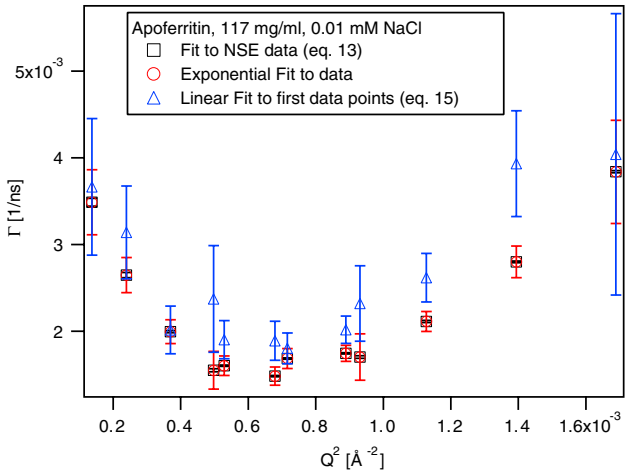

Fig. 5 Relaxation rates measured by NSE in solution with interparticle interactions being present (apoferritin concentration 117 mg/ml). In Fig. 5, the relaxation rates received by a single exponential fit and additional fits using Eqs. 15 and 17 are compared. The latter fit functions take into account the relative wavelength spread of 17%. The approximate fit values obtained by Eq. 17 show the largest error bars, and are found to be larger than the other fit values, but the difference remains smaller than the fit errors

points and consequently the fit ranges used in the two fitting methods are very different. For example, at the highest q-value shown, the linear fit is only applied to the first six data points. The difference at $q = 0.042$ Å^{-1} is explained by the fact that $S(q)$ is most different from a constant shape there.

Finally, we combine two dynamic measurements, to calculate the normalized inverse effective diffusion coefficient D_0/D_{eff}. The relaxation rates obtained by fitting the spin echo curves of an interacting protein solution with Eq. 17 are inversed and multiplied by the free-particle values, as shown in Fig. 2. In Fig. 6 (right), these dynamic data are compared with the structure factor data from Häußler (2003), on the linear q-scale. To improve statistics, the detected counts are grouped into only two sections. As expected (Pusey and Tough 1985), a maximum appears corresponding to the main $S(q)$ peak. For the concentration of 117 mg/ml shown here, the coincidence of the static and dynamic data is evident. However, the dynamic data are significantly found to be higher than the static data. This indicates the presence of indirect interactions in addition to the direct electrostatic forces, slowing down the dynamics.

Conclusions

We performed neutron scattering experiments on ferritin in solutions of various protein concentrations and salt contents. Hereby, ferritin serves as a model system, to study the differences between protein systems without and with interactions. Beyond delivering data for comparison with theory, our results point out the importance to correct results of other QENS measurements not only for free-particle diffusion, but also to take into account the specific dynamical picture present in interacting solutions. For analysis of the NSE data taking into acoount the wavelength spread used, we derive more sophisticated fit function than the usually used (single) exponential functions.

The study demonstrates that only at relatively low concentration and high ionic strength, the proteins show classical diffusion. This free-particle diffusion of ferritin is well described by the fit function taking into account the NSE wavelength spread (Eq. 13). The diffusion constant

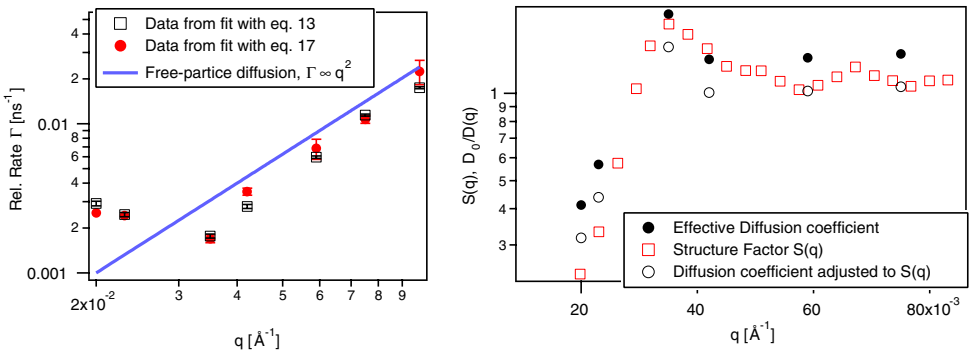

Fig. 6 *Left* Relaxation rates for the low-salt sample with apoferritin concentration of 117 mg/ml. At low q, the dynamics is much faster and the relaxation rate Γ does not follow the free diffusion dependency $\Gamma \sim q^2$. At intermediate q-values, the Γ-curve crosses the free-particle diffusion curve (*line*). Following the shape to higher q-values, the relaxation turns towards the free-particle diffusion line. *Right* The normalized inverse normalized effective diffusion coefficient $D_0/D_{\text{eff}}(q)$ is displayed together with the structure factor $S(q)$ calculated by division of the intensity data through the form factor (Eq. 7). There are no qualitative differences between the static and dynamic data. Position, height and shape of the peaks are similar, as seen by adjusting the relative values of $D_0/D_{\text{eff}}(q)$ to $S(q)$. The absolute values of $D_0/D_{\text{eff}}(q)$ (*solid circles*), however, are larger than the structure factor values

was found to agree with the size of the apoferritin shell and with literature.

The dynamic picture of the higher concentrated solutions as measured by NSE reflects the influence of both direct electrostatic and indirect interactions on the dynamics. At high q-values, the dynamics in solutions of higher protein concentration can be fitted well by a NSE fit function (Eq. 15), similarly to the low concentration data, At high q, the structure factor of all systems under study is nearly constant, so that Eq. 15 is valid. The results show that the diffusive dynamics are mainly decelerated indicating the existence of indirect interactions. For the systems at high ionic strength, the analysis of the influence of indirect interactions has been performed quantitatively, although the analysis was restricted to only three concentration values.

In solutions of low ionic strength, strong direct interactions reflected in the structure factor peak slow down the decay of the normalized intermediate scattering function, in addition to indirect interactions. Because of the slope of $S(q)$ near its peak, Eq. 15 is not valid any more, because NSE uses a broad wavelength band inducing averaging over a certain q-range (Eq. 11). Therefore, an approximate linear fit function has to be used here, and we restrict ourselves to study the correlation between static structure and dynamics near the structure factor peak qualitatively. For a quantitative analysis near the structure factor maximum, we will improve the fitting strategy in future work.

Acknowledgments We would like to thank B. Farago for setting up the instrument IN15, and the Institute Laue Langevin for the beam time given at this instrument.

References

Brown W (ed) (1996) Dynamic light scattering: the method and some applications. Clarendon Press, Oxford
Doster W, Cusack S, Petry W (1989) Nature 337:754
Häußler W (2003) Chem Phys 292:425–434
Harrison PM, Arosio P (1996) Biochim Biophys Acta 1275:161
Israelachvili J, Wennerstroem H (1996) Nature 379:219
Kilcoyne SH, Mitchell GR, Cywinski R (1992) Physica B 180/181:767
Lovesey SW (1986) Theory of neutron scattering from condensed matter, vol 1: nuclear scattering. Oxford University Press, Oxford
Mezei F (ed) (1980) Neutron spin echo. Springer, Berlin
Nägele G (2004) The physics of colloidal soft matter, lecture notes 14, Institute of Fundamental Technological Research. Polish Academy of Sciences Publication, Warsaw
Pusey PN, Tough RJA (1985) Particle interactions. In: Pecora R (ed) Dynamic light scattering. Plenum Press, New York, pp 85–179
Pedersen JS (1997) Adv Colloid Interface Sci 70:171
Petsev N, Vekilov PG (2000) Phys Rev Lett 84:1339
Sivergun DI, Richard S, Koch MHJ, Sayers Z, Kuprin S, Zaccai G (1998) Proc Natl Acad Sci USA 95:2267
Häußler W, Wilk A, Gapinski J, Patkowski A (2002) J Chem Phys 117:413
Gapinski J, Wilk A, Patkowski A, Häußler W, Banchio AJ, Pecora R, Nägele G (2005) J Chem Phys 123:054708
ILL Yellow Book (2007) http://www.ill.fr/YellowBook/IN15, cited 1 Oct 2007